Semiconductor Physics, Quantum Electronics & Optoelectronics, 2014. V. 17, N 4. P. 336-340.

PACS 78.67.Bf, 78.55.Ap

Nickel-induced enhancement of photoluminescence in nc-Si–SiO_x nanostructures

K.V. Michailovska, I.Z. Indutnyi, P.E. Shepeliavyi, V.A. Dan'ko
V. Lashkaryov Institute of Semiconductor Physics, NAS of Ukraine
41, prospect Nauky, 03028 Kyiv, Ukraine
E-mail: indutnyy@isp. kiev.ua

Abstract. The effect of nickel silicide interlayer on the intensity of photoluminescence (PL) from Si nanoclusters (nc) in normally deposited and obliquely deposited in vacuum SiO_x/Ni/Si structures have been studied using spectral and time-resolved PL measurements. It has been shown that the intensity of PL band in SiO_x/Ni/Si samples is essentially higher than that in reference SiO_x/Si samples (without the nickel interlayer) with the same characteristics and treatment. The PL intensity enhancement factor is equal to 5.77 for normally deposited samples and 18 for obliquely deposited samples. The unchanged spectral shape of PL bands and similar position of PL maximum in samples with and without nickel silicide interlayer indicates that in the SiO_x/Ni/Si structures after annealing no additional emitting centers are introduced to compare with reference one. Time-resolved measurements showed that PL decay rate was decreased from $8.2 \cdot 10^4$ s^{-1} for SiO_x/Si specimens to $2.86 \cdot 10^4$ s^{-1} for SiO_x/Ni/Si one. The emission decay rate distribution was determined by fitting the experimental decay curves to the stretched-exponential model. The observed narrow decay rate distribution, decrease of the PL decay rate and enhancement of the PL intensity in SiO_x/Ni/Si samples can be assigned to the processes of nickel silicide passivation of the dangling bonds at the interface of Si nanoparticles and the silicon oxide matrix, which is more effective in porous samples.

Keywords: time-resolved photoluminescence, thin film, silicon oxide, nanoparticle, nickel silicide.

Manuscript received 22.04.14; revised version received 16.07.14; accepted for publication 29.10.14; published online 10.11.14.

1. Introduction

Thin-film structures containing Si nanoparticles embedded into SiO_x matrix attract attention of many researchers because of their promising applications in advanced electronic and optoelectronic devices [1-5]. But in spite of intensive researches over the past years, the reported efficiencies of nc-Si–SiO_x light-emitting structures are still low and not high enough for practical application. The most important factors influencing the characteristics of PL are nanoparticle size and state of nanoparticle–SiO_x interface. The passivation of nonradiative states and defects at this interface is an essential requirement in order to increase the intensity of PL. Hydrogen passivation through standard forming gas annealing is impractical for device application because hydrogen is easy-to-dissociate at elevated temperatures, which leads to the invalidation of hydrogen passivation. The Si–SiO_x interface can be modified by chemical compounds of necessary composition. Such treating is the most efficient in porous structures. Recently [6, 7], we have proposed the method of porous nc-Si–SiO_x

light-emitting structure formation using oblique deposition of Si monoxide (SiO) in vacuum. The electron microscopy studies show that, during this deposition, SiO_x films with a porous (column-like) structure are formed. During high-temperature annealing of these films, the thermally stimulated formation of Si nanoinclusions occurs in a restricted volume of the SiO_x column. Because of free space (cavities) between the oxide column, the structures is more susceptible to chemical treatments, e.g., to treatment with HF solution or vapor [8]. As a result of HF vapor treatment, approximately 200-fold increase in the PL intensity is observed.

It was reported also [3] that introduction of thin nickel interlayer between SiO_x films and Si substrates results in enhancing of the PL intensity of SiO_x/Ni/Si structures by a factor of 4 in comparison with samples without any Ni interlayer. Using the examples of light-emitting diodes based on $SiO_{1.56}$/Ni/Si structures, it was shown that $NiSi_2$ distribution in $SiO_{1.56}$ film could improve turn-on voltage and give a benefit to the electroluminescence efficiency [3]. In this paper, we report the results of studying the nickel induced enhancement of PL emission in porous and solid nc-Si–SiO_x light-emitting nanostructures.

2. Experimental

A thin (~12 nm) layer of Ni film was deposited by thermal evaporation of nickel powder onto (100)-oriented Si wafer. After deposition, the samples were annealed in vacuum at 450 °C for 10 min. The annealing provides the required energy for the system to overcome the energy barriers for solid state reaction of formation of intermediate nickel silicides [5]. Then, silicon oxide (SiO_x) film was deposited onto the nickel silicide film by thermal evaporation of Cerac. Inc. SiO with 99.9% purity in the vacuum chamber (the residual pressure $(1...2)\cdot 10^{-3}$ Pa). Before SiO_x deposition, the substrates were oriented at the angles (α) of 60° or 0° (normal deposition) between the normal to the substrate surface and direction to the evaporator. Because of the additional oxidation by residual gases during evaporation of SiO the compositionally nonstoichiometric SiO_x (x ~1.25 for normal deposition and x ~1.54 for 60°) films were obtained. The thickness of the SiO_x films were monitored *in situ* by the quartz-crystal-oscillator monitor system (KIT-1) and measured after deposition by a microinterferometer (MII-4). The thickness of normally deposited SiO_x films was equal to 400 nm, deposited at 60° – 700…800 nm. The samples without Ni interlayer were used as the reference ones in these measurements. As-deposited samples with and without Ni film were annealed simultaneously in vacuum at the temperature 975 °C for different duration ranging from 4 to 15 min. This high-temperature annealing leads to decomposition of silicon oxide (where x changed from 1.25 to 1.95 for samples obtained under normal deposition and from 1.54 to 2.0 for 60° ones) and formation of Si nanoparticles embedded into such oxide matrix [9, 10]. (The composition of the oxide matrix in as-deposited and annealed samples (parameter x) were determined using compositional dependence of the position of the main IR band in spectra of SiO_x layers within the range of 1000 to 1100 cm^{-1}, as it was ascertained in [11]. This band corresponds to the Si–O–Si stretching mode. FTIR measurements were carried out with Perkin-Elmer Spectrum BXII spectrometer.)

The structure of obliquely deposited SiO_x films was studied in our previous paper [12] by SEM apparatus ZEISS EVO 50XVP. Such SiO_x films have a porous inclined column-like structure with the column diameters of 10 to 100 nm. The porosity of films depends on the angle of deposition and equals to ~40% for $\alpha = 60°$. High-temperature annealing of these films does not change the porosity and column-like structure of the samples [7].

The PL spectra of obtained SiO_x/Ni/Si and SiO_x/Si samples were recorded at room temperature within the wavelength range 440 to 900 nm by using a system based on ZMR-3 monochromator equipped with a photomultiplier and detection system. The PL spectra were normalized to the spectral sensitivity of the experimental setup. The 337-nm line of a nitrogen laser with a spot size of about 2 mm in diameter was employed to excite the PL. Decay curve measurements were performed using the same N_2 laser with the pulse duration 9 ns, which was short as compared to PL average lifetimes of our samples (approximately tens of microseconds). The PL lifetime was measured at different emission wavelengths. The time trace was recorded with a resolution of 0.5 μs.

3. Results and discussion

Fig. 1 presents the PL spectra of normally deposited SiO_x/Ni/Si samples after annealing at 975 °C for 15 and 4 min (curve *1* and *2*, accordingly). Fig. 1 shows also PL spectra of the reference normally deposited SiO_x/Si sample (curve *3*) under annealing at the same temperature for 15 min. At room temperature, all the samples exhibited a broad band with a maximum of emission centered within 760…780 nm. This strong near-infrared luminescence band within the wavelength range 600…900 nm is associated with quantum confinement effects, that is with electron-hole pairs (or exciton) recombination in nc-Si. The intensity of emission from SiO_x/Ni/Si samples I_{PL}(Ni) is enhanced significantly in comparison with the reference sample (I_{PL}) and depends on the annealing time. So, the PL enhancement factor $\eta = I_{PL}(\mathrm{Ni})/I_{PL}$ measured at 780 nm increases from 2.45 to 5.77 for 4- and 15-min annealing time, accordingly.

Fig. 2 shows the PL spectra for the SiO_x/Ni/Si (curve *1*) and SiO_x/Si (curve *2*) samples deposited at 60° and annealed at 975 °C for 15 min in vacuum. The

emission spectrum of both samples exhibit a broad band with the peak position at 630 nm. A spectral shift of PL peaks to shorter wavelengths in obliquely deposited samples in comparison with normally deposited ones can be caused by decrease in nc-Si dimensions. The size of nc-Si in these systems depends on the silicon content in deposited SiO_x layers [13]: decrease in the Si content (i.e., increase of x) results in decreased nc-Si sizes and blue shift of PL spectrum. Besides, during high-temperature annealing of porous films with column-like structure the thermally stimulated formation of nc-Si occurs in a restricted volume of the SiO_x columns. It can also cause the reduction of the nc-Si size and blue shift of the PL peak.

As seen from Figs 1 and 2, addition of Ni interlayer results in enhancement of the PL intensity more prominent in porous samples. For porous, obliquely deposited samples, the enhancement factor η measured at 630 nm is equal to 18.

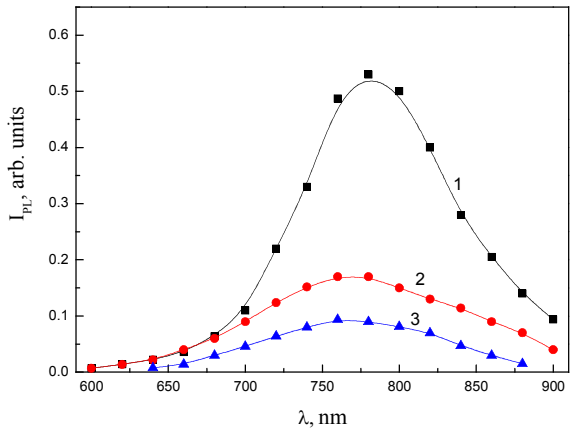

Fig. 1. PL spectra of normally deposited samples: SiO_x/Ni/Si after annealing in vacuum at 975 °C for 15 (*1*) and 4 min (*2*) and the reference SiO_x/Si sample after annealing at 975 °C for 15 min (*3*).

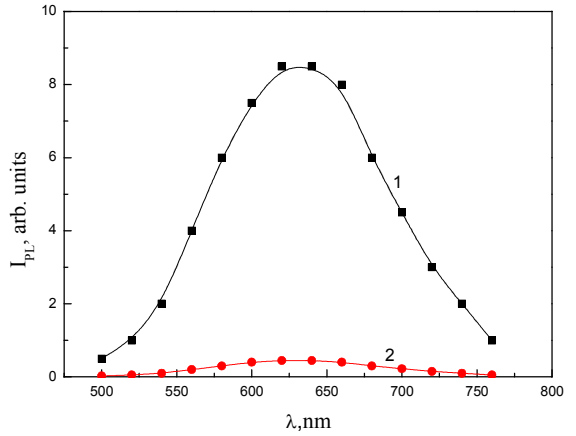

Fig. 2. PL spectra of SiO_x/Ni/Si (*1*) and reference of SiO_x/Si (*2*) samples obliquely deposited at the angle 60° after annealing in vacuum at 975 °C for 15 min.

It is known that, in a low excitation regime, the PL intensity is generally given by the expression $I_{PL} \sim (\tau_{PL}/\tau_R)\sigma\varphi N$, where τ_{PL} and τ_R are the photoluminescence and radiative lifetimes, respectively, φ is the photon flux of the laser pump (constant throughout our experiment), N is the density of nanocrystals in the film, and σ is their excited cross-section [17]. The unchanged spectral shape of PL bands and similar position of PL maximum in samples with and without Ni interlayer mean that in the SiO_x/Ni/Si structures after annealing no additional emitting centers are introduced to compare with the reference one. In the quantum confinement scheme, the light emission from nc-Si is caused by radiative recombination of electron-hole pairs (or excitons) confined within nanoparticle [15]. It is deduced that the radiative lifetimes τ_R would be close to each other in SiO_x/Ni/Si and SiO_x/Si samples due to the same luminescence scheme and similar size of nc-Si (similar position of the PL maximum). One can suppose that nc-Si density (N) and PL lifetime (τ_{PL}) are the main factors changing the PL intensity in SiO_x/Ni/Si samples. More direct demonstration of enhanced electron-hole pair recombination involved comparative measurements of the PL decay rate in the investigated structures.

Time-resolved PL measurements were performed using the normally deposited SiO_x/Ni/Si and SiO_x/Si samples. Fig. 3 shows PL decay curve for SiO_x/Ni/Si (curve *1*) and SiO_x/Si (curve *2*) samples at 780 nm. One can see that the PL intensity for the SiO_x/Ni/Si samples decayed slower than for the reference samples. The obtained decay curves of the PL intensity may be described well by a stretched exponential function:

$$I_{PL}(t) = C t^{\beta-1} \exp\left[-\left(\frac{t}{\tau_0}\right)^{\beta}\right], \qquad (1)$$

where C, τ_0 and β are some constant, decay time and stretched parameter ($0 < \beta \le 1$), respectively. It is known that the stretched exponential function is widely used for the decay curve analysis of Si nanocrystals [16]. The least-squares fit of Eq. (1) to experimental data brings values of τ_0 and β. The obtained decay times τ_0 were equal to 35 and 12.2 μs for SiO_x/Ni/Si and SiO_x/Si samples, respectively. This range of PL lifetimes is comparable with those reported in the literature for silicon nanocrystals at room temperature [17]. The PL decay rate $k\left(k = \tau_0^{-1}\right)$ at 780 nm is decreased from $8.2 \cdot 10^4$ s^{-1} for SiO_x/Si to $2.86 \cdot 10^4$ s^{-1} for SiO_x/Ni/Si samples. It was also determined that the dispersion parameter β is 0.83 for SiO_x/Ni/Si and 0.74 for SiO_x/Si samples. In general, the parameter β is related to the stretching of the decay process and is a direct measure of the width of the decay rate distribution. In the case of stretched exponential relaxation function, the PL decay may be analyzed more thoroughly by recovering the distribution of recombination rates [16].

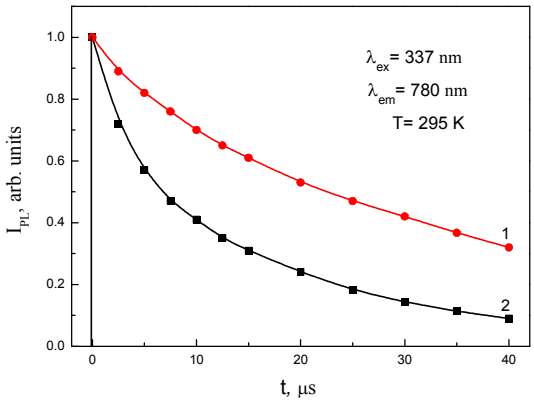

Fig. 3. PL decay curves measured at 780 nm for the normally deposited SiO_x/Ni/Si (*1*) and SiO_x/Si (*2*) samples after annealing at 975 °C for 15 min.

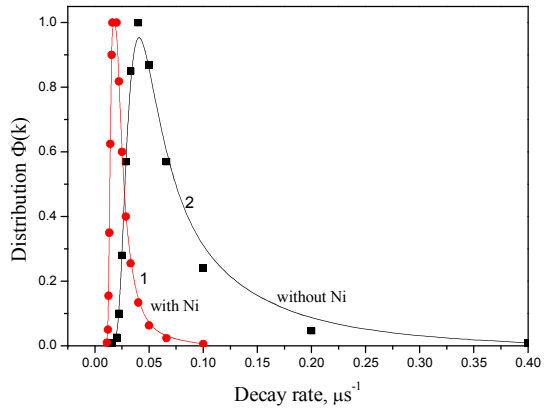

Fig. 4. Decay rate distributions of SiO_x/Ni/Si (*1*) and SiO_x/Si (*2*) normally deposited samples obtained from the stretched-exponential decay model. The decay rate distributions are normalized by the peak value of $\Phi(k)$ for both samples.

Using the values of τ_0 and β measured at $\lambda =$ 780 nm, we calculated the asymptotic form of the decay rates probability density function $\Phi(k)$ that might be obtained by the saddle-point method [18]:

$$\Phi(k) = \frac{a\tau}{\sqrt{2\pi\beta}} \cdot (k\tau)^{-1-a/2} \cdot \exp\left[-(k\tau)^{-a}\right], \qquad (2)$$

where $a = \beta(1-\beta)^{-1}$ and $\tau = \tau_0\left[\beta(1-\beta)^{1/a}\right]^{-1}$. Fig. 4 shows the $\Phi(k)$ distributions calculated from Eq. (2) for SiO_x/Ni/Si (curve *1*) and SiO_x/Si (curve *2*) samples. The obtained distribution for the reference SiO_x/Si sample is very broad with a long tail directed towards shorter lifetimes, which demonstrates the strongly non-single exponential character of decay curves. In SiO_x/Ni/Si samples, the decay rate distribution $\Phi(k)$ is more narrow as compared with SiO_x/Si sample and shifts towards lower decay rates. To explain the observed feature, it should be mentioned that the obtained $\Phi(k)$ function provides information about both the radiative (k_R) and nonradiative (k_{NR}) relaxation rates [19]. A very low quantum efficiency of nc-Si emission suggests that nonradiative processes should be predominant ($k_{NR} >> k_R$). It allows us to relate the changes observed in the decay rate distribution $\Phi(k)$ to the different quantity of defect states (dangling silicon bonds) in the matrix containing nc-Si. We believe that the interface between nc-Si and the SiO_x matrix plays a crucial role in distributing decay rates [20]. SiO_2 is an ideal matrix for nc-Si, as it can passivate a large fraction of the dangling Si bonds. There is a remarkable content of broken silicon bonds in SiO_x films, which may act as nonradiative recombination paths for the excited carriers and cause the quenching of PL [21]. The observed narrow decay rate distribution and the increase of the PL decay time in SiO_x/Ni/Si samples can be related to the processes of nickel silicide passivation of nonradiative recombination centers. It has been reported previously that nickel silicide thin films were formed by vacuum thermal processing (350-750 °C) of Ni thin films deposited onto (100) *p*-type Si substrates [4]. Ni as the mobile species moves through NiSi during the transition from NiSi to the $NiSi_2$ phase at 750…1000 °C [22]. $NiSi_2$ distributed in SiO_x film passivates the broken bonds on the nc-Si surface [23]. The model of $NiSi_2$ passivation was proved by thermodynamic analysis and Fourier transform infrared spectroscopy in $SiO_{1.56}$/Ni/Si systems [3].

In the porous SiO_x/Ni/Si samples, the nickel diffusion processes significantly accelerated due to the presence of voids and the surface of nanocolumns. This leads to more effective passivation of the nonradiative recombination centers and more significant increase in the PL emission intensity.

In conclusion, we can note that the PL intensity enhancement factor calculated from the experimental results for SiO_x/Ni/Si and SiO_x/Si samples annealed at 975 °C is $\eta = 5.77$ for normal deposited samples. Enhancement of PL lifetimes in these samples by the factor ~2.87 due to the processes of nickel silicide passivation is not enough for explanation of the increase in PL intensity. Therefore, we proposed that the PL intensity enhancement can be caused both by increasing the PL lifetime and also by increasing the nc-Si density. The presence of Ni gives an additional driving force to the separation process of SiO_x which was discussed in the previous paper [24].

5. Conclusion

In summary, we have presented the effect of Ni on the PL emission from Si nanoparticles embedded in the silicon oxide matrix. It has been shown that the intensity of near-infrared emission band in SiO_x/Ni/Si samples was significantly higher than that in the samples without the Ni interlayer. It was assumed that nickel in SiO_x film may passivate the residual dangling bonds at the interface of nc-Si and SiO_x matrix. Time-resolved PL measurements showed the decrease in the PL decay rate in SiO_x/Ni/Si samples as compared with the SiO_x/Si one. Decrease in the PL decay rate and increase in the density

of nc-Si could be the main factors enhancing the PL intensity in nanostructures with nickel silicide interlayer.

References

1. K.S. Min, K.V. Shcheglov, S.M. Yang, H.A. Atwater et al., Defect related versus excitonic visible light emission from ion beam synthesized Si nanocrystals // *Appl. Phys. Lett.* **69**, p. 2033-2035 (1996).
2. M. Fujii, A. Mimura, S. Hayashi, K. Yamammoto et al., Improvement in photoluminescence efficiency of SiO_2 films contaning Si nanocrystals by P doping // *J. Appl. Phys*. **87**, p. 1855-1857 (2000).
3. D.X. Li, Y. He, J.Y. Feng, The study of nickel-induced enhancement of near-infrared luminescence in Si-rich silicon oxide films // *Physica E*, **41**, p. 812-816 (2009).
4. M. Tinani, A. Mueller, Y. Gao et. al., *In situ* real-time studies of nickel silicide phase formation // *J. Vac. Sci. Technol*. *B*, **19**(2), p. 376-383 (2001).
5. F.F. Zhao, J.Z. Zheng, Z.X. Shen et al., Thermal stability of NiSi and $NiSi_2$ thin films // *Microelectron. Eng.* **71**(1), p. 104-111 (2004).
6. I.Z. Indutnyy, I.Yu. Maidanchuk, V.I. Min'ko, Visible photoluminescence from annealed porous SiO_x films // *J. Optoelectron. and Adv. Mater.* **7**, p. 1231-1236 (2005).
7. V.A. Dan'ko, I.Z. Indutnyy, I.Y. Maidanchuk et al., Formation of the photoluminescence structure based on SiO_x porous films // *Optoelektronika i poluprovodnikovaya tekhnika*, **39**, p. 65-72 (2004) (in Ukrainian).
8. I.Z. Indutnyi, E.V. Michailovskaya, P.E. Shepeliavyi and V.A. Dan'ko, Visible photoluminescence of selectively etched porous nc-Si–SiO_x structures // *Fizika tekhnika poluprovodnikov* **44**(2), p. 218-222 (2010) (in Russian) [*Semiconductors*, **44**(2), p. 206-210 (2010)].
9. V.A. Dan'ko, V.Ya. Bratus', I.Z. Indutnyi, I.P. Lisovskyy, S.O. Zlobin, K.V. Michailovska, P.E. Shepeliavyi, Controlling the photo-luminescence spectra of porous nc-Si–SiO_x structures by vapor treatment // *Semiconductor Physics, Quantum Electronics & Optoelectronics*, **13**(4). p. 413-417 (2010).
10. V.Ya. Bratus', V.A. Yukhimchuk, L.V. Berezhinsky et al., Structural transformation and silicon nanocrystallite formation in SiO_x films // *Semiconductors*, **35**(7), p. 821-826 (2001).
11. M. Nakamura, Y. Mochizuki, K. Usami et al., Infrared absorption spectra and compositions of evaporated silicon oxide (SiO_x) // *Solid State Communs.* **50**, p. 1079-1081 (1984).
12. I.Z. Indutnyi, K.V. Michailovska, V.I. Min'ko, P.E. Shepeliavyi, Effect of acetone vapor treatment on photoluminescence of porous nc-Si–SiO_x nanostructures // *Semiconductor Physics, Quantum Electronics & Optoelectronics*, **12**(2), p. 105-109 (2009).
13. D. Nesheva, C. Raptis, A. Perakis et al., Raman scattering and photoluminescence from Si nanoparticles in annealed SiO_x thin films // *J. Appl. Phys.* **92**, p. 4678-4683 (2002).
14. C. Garcia, B. Garrido, P. Pellegrino et al., Size dependence of lifetime and absorption cross section of Si nanocrysrals embedded in SiO_2 // *Appl. Phys. Lett*. **82**, p. 1595-1597 (2003).
15. C. Delerue, G. Allan, M. Lannoo, Theoretical aspects of the luminescence of porous silicon // *Phys. Rev. B*, **48**, p. 11024-11036 (1993).
16. G. Zatrub, A. Podhorodecki, J. Misiewicz et al., On the nature of the stretched exponential photoluminescence decay for silicon nanocrystals // *Nanoscale Res. Lett*. **6**, p. 106 (2011).
17. M. Dovrat, Y. Goshen, J. Jedrzejewski, I. Balberg, A. Sa'ar, Radiative versus nonradiative decay process in silicon nanocrystals probed by time-resolved photoluminescence spectroscopy // *Phys. Rev. B*, **69**, 155311 (2004).
18. R. Sato, K. Murayama, A universal distribution function of relaxation in amorphous materials // *Solid State Communs*. **63**, p. 625-627 (1987).
19. A.F. van Driel, I.S. Nikolaev, P. Vergeer et al., Statistical analysis of time-resolved emission from ensembles of semiconductor quantum dots: interpretation of exponential decay models // *Phys. Rev. B*, **75**, 035329 (2007).
20. G. Hadjisavvas, P.C. Kelires, Structure and energetics of Si nanocrystals embedded in α-SiO_2 // *Phys. Rev. Lett*. **93**, p. 226104 (2004).
21. I. Mihalcescu, J.C. Vial, R. Romestain, Carrier localization in porous silicon investigated by time-resolved luminescence analysis // *J. Appl. Phys*. **80**, p. 2404 (1996).
22. M. Bhaskaran, S. Sriram, T.S. Perova et al., *In situ* micro-Raman analysis and X-ray diffraction of nickel silicide thin films on silica // *Micron*, **40**(1), p. 89-93 (2009).
23. H.F. Yan, Y.J. Xing, Q.L. Hang, D.P. Yu, Y.P. Wang et al., Growth of amorphous silicon nanowires via a solid-liquid-solid mechanism // *Chem. Phys. Lett*. **323**, p. 224-228 (2000).
24. Y. He, K. Ma, I. Bi, J.Y. Feng, Z.J. Zhang, Nickel-induced enhancement of photoluminescence from Si-rich silica films // *Appl. Phys. Lett*. **88**, 031905 (2006).